Available online at www.sciencedirect.com
SCIENCE DIRECT
Journal of Solid State Chemistry 179 (2006) 1924–1930
JOURNAL OF SOLID STATE CHEMISTRY
www.elsevier.com/locate/jssc

Rapid communication

Preferential occupation of alkaline-earth metal sites in a seemingly disordered solid solution of $Ca_{11-x}Sr_xSb_{10}$: Single crystal structures of $Ca_{8.63(5)}Sr_{2.37}Sb_{10}$ and $Ca_{3.66(7)}Sr_{7.34}Sb_{10}$

Shalabh Gupta[a], Ashok K. Ganguli[a,b,*]

[a]Department of Chemistry, Indian Institute of Technology Delhi, Hauz Khas, New Delhi 110016, India
[b]Visiting Scientist, Department of Chemistry, Iowa State University, Ames, IA 50011, USA

Received 24 January 2006; received in revised form 14 March 2006; accepted 19 March 2006
Available online 28 March 2006

Abstract

Two new antimony based intermetallic phases, $Ca_{8.63(5)}Sr_{2.37}Sb_{10}$ **(1)** and $Ca_{3.66(7)}Sr_{7.34}Sb_{10}$ **(2)**, crystallizing in $Ho_{11}Ge_{10}$ structure type (tetragonal, $I4/mmm$) have been synthesized and characterized. Although both $Ca_{11}Sb_{10}$ and $Sr_{11}Sb_{10}$ are known to be isostructural ($Ho_{11}Ge_{10}$ structure type) and hence all Ca sites should be accessible to Sr as well, it appears that certain sites are preferentially ordered by Ca in the mixed $(Ca/Sr)_{11}Sb_{10}$ compounds reported here. The crystal structure of $Ca_{8.63(5)}Sr_{2.37}Sb_{10}$ and $Ca_{3.66(7)}Sr_{7.34}Sb_{10}$ has been solved from single crystal X-ray data using direct methods and refined using full-matrix least-squares method. The structure can be described as bonded network of A-Sb (A = Ca, Sr) with Sb existing as isolated Sb^{3-}, diantimony Sb_2^{4-} and Sb_4^{4-} square units. Simple valence electron count reveals these compounds to be Zintl phases. It is found that the larger Sr or Sr/Ca ions preferentially occupy sites that are closer to the diantimony anions as compared to the smaller Ca ions.

Keywords: Antimonide; Crystal structure; $Ho_{11}Ge_{10}$ structure; Antimony dimers; Magnetic susceptibility

1. Introduction

Intense exploratory research in the area of polar intermetallics has led to an ever increasing number of unprecedented and interesting structure types [1–3]. New compounds in previously known structure types do result more often providing a better understanding of bonding and stability of a structure. This understanding provides the researchers with a scope to tailor the electronic properties and explore more into the material aspects of these compounds. Polar intermetallics are formed with electropositive elements (alkali and alkaline earth) and the elements on the Zintl border (groups 13–15). They display a rich variety of structural features and novel electronic properties that require understanding of new concepts like metallic Zintl phases [4,5] and the effect of packing and non-classical bonding [6–8]. The nature of these compounds is such that they combine the properties of a true intermetallic and a valence compound. In other words they display a pronounced heteropolar bonding contribution (cation–anion interaction) and at the same time their anionic partial lattice obeys the 8-N rule as given by the Zintl-Klemm principle. It has been indicated in literature [9] that the stabilities of these ionic cluster salts are influenced by packing and electronic effects. Cations play an important role in stabilizing the anionic cluster species through appreciable lattice covalency. The electronegativity difference between the bonding atoms being intermediate between those found in the intermetallic and the ionic compounds, rich bonding patterns which are not so obvious are often encountered. In the absence of an incomplete electron transfer from the more electropositive element to the less electropositive element and the necessity to achieve a closed-shell configuration, homoatomic bonding takes place. Various examples known in the literature

*Corresponding author. Department of Chemistry, Indian Institute of Technology Delhi, Hauz Khas, New Delhi 110016, India.
Fax: +91 11 26854715.
E-mail address: ashok@chemistry.iitd.ernet.in (A.K. Ganguli).

0022-4596/$ - see front matter © 2006 Elsevier Inc. All rights reserved.
doi:10.1016/j.jssc.2006.03.027

indicate that in the absence of sufficient number of electrons appreciable interanionic interactions set in [10,11]. Among the several families of polar intermetallics the antimonides have been of interest lately due to the possibility of finding interesting thermo-electric materials [12,13]. In this article we report two mixed alkaline-earth metal antimonide ($Ca_{8.63(5)}Sr_{2.37}Sb_{10}$ **(1)** and $Ca_{3.66(7)}Sr_{7.34}Sb_{10}$ **(2)**) crystallizing in $Ho_{11}Ge_{10}$ structure type [14] with distinct site preference for the two cations (Ca, Sr) which differ in size. It is interesting to note that though both the end members $Ca_{11}Sb_{10}$ [15] and $Sr_{11}Sb_{10}$ [16] are known, still there is a definite preference of some sites for the smaller (Ca) ions as compared to the larger (Sr) ions. Both **(1)** and **(2)** have three types of anionic species: Sb_4 (2-bonded) square planar rings, Sb_2 (1-bonded) dumbells and monoatomic Sb. Following the 8-N formulation the charges assigned to these species, 4-, 4- and 3-, respectively, makes these compounds an electron precise Zintl phase. Sb_2 and Sb_4 are the most commonly encountered substructures with the bond length ranging from 2.80 to 2.90 Å for the former. A recently reported examples in $A_2Ca_{10}Sb_9$ (A = Li, Mg) [17] system displayed isolated cations of alkaline-earth metals interbonded with isolated Sb^{3-} and Sb_2^{4-} dimers described in terms of two slab types stacked along c. The arrangement of Sb_2 dimers was found to be very similar to that found in antimonides crystallizing in $Ho_{11}Ge_{10}$ structure type [14]. Several pnictides though relatively few, have been reported in the $Ho_{11}Ge_{10}$ structure type, $Eu_{11}Sb_{10}$ [18] and $Yb_{11}Sb_{10}$ [19] being the earliest and the only known rare-earth analogs.

2. Experimental section

2.1. Syntheses

Single crystals of **(1)** and **(2)** were obtained by reacting the high purity elements (Dendritic Ca (99.8%, Alfa-Aesar), Sr chunks (99.8%, Alfa-Aesar) and Sb chunks (99.99%, Johnson–Matthey) at high temperature in a sealed (1/4 in. diameter Ta) metal tubing. Elements were loaded into these metal containers inside a He-filled glovebox. The tubes were welded and jacketed in evacuated and baked fused-silica containers, and heated in resistance furnaces. Crystals of **(1)** were obtained from a reaction mixture with composition of $Ca_2MgSrSb_4$ and heated at 850 °C for 2 h followed by annealing at 300 °C for 5 days. Crystals of the Sr rich phase **(2)** were obtained during an attempt to obtain other phases in $Ca_{11-x}Sr_xSb_{10}$ series from a reaction mixture with the loaded composition of $Sr_{5.5}Ca_{5.5}Sb_{10}$. Various other compositions were loaded in this series. A quick analysis of the products obtained from reactions containing Mg, Ca, Sr and Sb in various ratios reveal that the 11:10 phase appears only for Sb/A ratio $\geqslant 1$. Reactions loaded with Mg mixed either with Ca or Sr under at least two different conditions did not yield the magnesium containing $A_{11}Sb_{10}$ phase in any case. Instead, Mg_2ASb_2 (A = Ca, Sr) formed as a major phase along with Ta_5Sb_3 in minor proportions. Refinement of **(1)** suggested one mixed cation site with Sr:Ca ratio of ~30:70. However the structure could be refined equally well with Sr:Mg ratio of ~50:50. We assume the site to contain only Ca and Sr, the assumption being based on the presence of another Mg containing phase $SrMg_2Sb_2$. These phases were identified via Guinier patterns obtained from a Huber 670 powder camera; details of the procedures have been described before [20]. Two sets of three compositions covering a broad span of solid solution $Ca_{11-x}Sr_xSb_{10}$ ($x = 3.5$, 5.5 and 7.5) were heated under two conditions in order to obtain pure phases. The results obtained are given in Table 1.

Thus under these conditions (Table 1) pure phases could be obtained only when the loaded Ca concentration is less than or equal to the loaded Sr concentration. For higher Ca concentrations ($x < \sim 5.5$ and below), the pure Ca-phase $Ca_{16}Sb_{11}$ [21] formed more readily. From our above studies it appears that **(2)** is a congruently melting phase while **(1)** may be an incongruently melting phase since on loading the Ca-rich composition, $Ca_{7.5}Sr_{3.5}Sb_{10}$ leads to a biphasic mixture of $Ca_{16}Sb_{11}$ and another unknown phase. Note that the single crystals of the Ca-rich composition, $Ca_{8.63(5)}Sr_{2.37}Sb_{10}$ were obtained from a loaded composition, $Ca_2MgSrSb_4$.

2.2. Structural studies

Several irregular crystals were selected from the reaction mixture and saved in thin-wall glass capillaries inside a N_2 filled glovebox designed for this purpose. After examining each crystal, data sets were collected (at room temperature) on suitable crystals on a Bruker APEX CCD diffractometer equipped with a Mo$K\alpha$ fine-focus sealed tube ($\lambda = .71073$ Å) and a graphite monochromator. Data collection was carried out over a Θ range of ~2.09 to 28.27°. The detector was placed at a distance of 5.995 cm from the crystal. For both the crystals of **(1)** and **(2)**, three sets of 600 frames were collected with a scan width of .3° in

Table 1
Reaction conditions and phases obtained

Loaded composition	Phase analysis (powder X-ray diffraction)
$Ca_{3.5}Sr_{7.5}Sb_{10}$[a]	$A_{11}Sb_{10}$-type, single phase powder pattern matches well with **(2)**
$Ca_{5.5}Sr_{5.5}Sb_{10}$[a]	$A_{11}Sb_{10}$-type, appears single phase with larger Sr content than **(1)** but lower than **(2)**
$Ca_{7.5}Sr_{3.5}Sb_{10}$[a]	$Ca_{16}Sb_{11}$ [19] (90%) + unknown phase
$Ca_{3.5}Sr_{7.5}Sb_{10}$[b]	$A_{11}Sb_{10}$-type, nearly single phase powder pattern matches well with **(2)**
$Ca_{5.5}Sr_{5.5}Sb_{10}$[b]	$A_{11}Sb_{10}$-type, (~90%) powder pattern matches well with **(2)** + $Ca_{16}Sb_{11}$(shifted d-values) ~10%
$Ca_{7.5}Sr_{3.5}Sb_{10}$[b]	$Ca_{16}Sb_{11}$(shifted) + $A_{11}Sb_{10}$-type (shifted d-values)

[a]950 °C/2 days/ cool at 5 °C/h.
[b]950 °C/1 day/quench; anneal 600 °C/7 days cool at 5 °C/h.

ω and an exposure time of 10 s per frame. The frames were integrated with the SAINT program in the SMART software package [22] using a narrow-frame integration algorithm. Data were corrected for absorption effects using the multi-scan technique using SADABS [22].

The crystal structures were solved and refined using the SHELXTL (Version 6.1) Software Package [23]. For **(1)**, out of the several suggested body centered space groups consistent with the extinctions, refinement was attempted in the $I4/m$ (No. 87) and $I4/mmm$ (No. 139) space groups. The preliminary choice for the space group was based on the mean E^2-1 value that was close to the expected value for the centrosymmetric space group and a reasonable combined figure of merit, with $Z=4$. The latter ($I4/mmm$ space group) was selected for the refinement and the satisfactory solution of the structure by direct methods and its final refinement affirmed this selection. No systematic absence violations or inconsistent equivalents were observed in any of these data sets. The structure was solved with SHELXS [23] using direct methods and refined by full matrix least-squares refinements on F_0^2.

Some collection and refinement parameters in the standard settings for both **(1)** and **(2)** are given in Table 2, and more complete details as well as the final anisotropic displacement parameters are contained in the Supporting Information. The final positional parameters and isotropic-equivalent displacement ellipsoids for all atoms in both the compounds are collectively given in Table 3. The initial model for **(1)** suggested 3 Sb sites and 6 alkaline-earth metal sites of which two were assigned as Sr and rest as Ca. Refinement with this model for a few cycles revealed all the positions to be correct. However a strong residual appeared close to one of the Sr atom on refining the thermal parameters anisotropically. This position was subsequently refined as Sb4. The main problem during the refinement appeared with the prospective Sb5 position ($8h$), which was assumed to be Ca in the initial solution. On refining this position as Sr lead to a U_{eq} value of $38(1)\times10^{-3}$ Å^2. Refinement of the occupancy suggested a heavier Sb to be the more appropriate element, which refined with ~7% deficiency but still had a large U_{eq} of 52×10^{-3} Å^2. Among the alkaline-earth metal sites, one of the sites (A1), suggested as Ca in the initial model, refined with very low U_{eq} value of $62(9)\times10^{-4}$ Å^2. Replacing Ca with Sr led to a high isotropic thermal parameter which on subsequent occupancy refinement indicated only ~60% site occupancy. Further refinement of this site with mixed-cation (Ca and Sr) occupancy led to a satisfactory thermal parameter with Sr:Ca ratio of 35:65. Another alkaline-earth metal site ($A3$), refined with high U_{eq} value of $59(2)\times10^{-3}$ Å^2. Occupancy refinement suggested the site to be ~94% occupied by Ca, which compared well with the deficiency of Sb at Sb5 position and thereby maintaining the electron precise nature of these Zintl phases. This however led only to a marginal improvement in the thermal parameter of this Ca site and accordingly site occupancies for both these sites were set to 100% in the final refinement.

Table 2
Single crystal data collection and refinement parameters

Empirical formula	$Ca_{8.63}Sr_{2.37}Sb_{10}$	$Ca_{3.66}Sr_{7.34}Sb_{10}$
Formula weight	1771.03	2007.31
Temperature (K)	298(2)	298(2)
Wavelength (Å)	.71073	.71073
Crystal system	Tetragonal	Tetragonal
Space group	$I4/mmm$	$I4/mmm$
Unit cell dimensions (Å)	$a=12.0458(8)$	12.3498(8)
	$c=17.501(2)$	17.767(2)
Volume (Å^3), Z	2539.5(4), 4	2709.8(4), 4
Density (calculated) (mg/m^3)	4.241	4.835
Absorption coefficient (mm^{-1})	21.613	24.368
$F(000)$	2834	3391
Crystal size (mm^3)	$.07\times.06\times.06$	$.09\times.06\times.05$
Theta range for data collection	2.05–28.28°	2.01–28.21°.
Index ranges	$-15\leqslant h\leqslant14$, $-15\leqslant k\leqslant15$, $-22\leqslant l\leqslant19$	$-13\leqslant h\leqslant16$, $-16\leqslant k\leqslant14$, $-23\leqslant l\leqslant13$
Refinement method	Full-matrix least-squares on F^2	
Data/restraints/parameters	914/0/40	997/0/42
Goodness-of-fit on F^2	1.089	1.011
Final R indices $[I>2\sigma(I)]$	$R_1=.0453$, $wR_2=.0952$	$R_1=.0369$, $wR_2=.0628$
R indices (all data)	$R_1=.0551$, $wR_2=.0988$	$R_1=.0636$, $wR_2=.0709$
ρ_{max}/ρ_{min} (e Å^{-3})	5.669/−3.682	2.91/ − 2.87

$R_1=\Sigma(|F_o|-|F_c|)/\Sigma(|F_o|)$. $wR_2=[\Sigma w(F_o^2-F_c^2)/\Sigma wF_o^4]^{1/2}$. GOF $=[\Sigma w(F_o^2-F_c^2)/(n-p)]^{1/2}$ where n is the number of reflections and p is the number of parameters refined.

Refinement of rest of the alkaline-earth metal sites ($A2$ and $A4$) was uneventful. High-thermal parameters for Sb5 were also observed in $Sr_{11}Sb_{10}$ [16], $Sr_5Ba_6Sb_{10}$ [24], and the bismuth analogues $Sr_{11}Bi_{10}$ and $Ba_{11}Bi_{10}$ [24]. The authors in these cases had verified the actual composition using EDAX and also observed it as a general anomaly for $Ho_{11}Ge_{10}$ structure type. Though in none of the earlier reports [16,24], this deficiency in the Sb5 position been reported, we believe that there is a genuine deficiency of Sb (~7%) at this site as indicated by the small errors involved with the refined occupancy and failure to get a better solution in lower symmetry space groups. This deficiency may however be accompanied by a similar deficiency in some cation site as indicated above, thus preserving the electron precise nature of these compounds. A more detailed analysis of the Sb5 thermal parameter is given in the results and discussion. The structure refinement for **(2)** proceeded in a similar fashion and also led to a high value of U_{eq} for Sb5. Occupancy refinement once again lead to some vacancy in this site. This however did not lead to any appreciable change in any of the interatomic distances and thus would not lead to any appreciable change in our arguments on the site preferences. The final anisotropic

Table 3
Atomic coordinates ($\times 10^4$) and equivalent isotropic displacement parameters ($Å^2 \times 10^3$)

Atom	Wyckoff	x	y	z	U_{eq}	Occupancy
$Ca_{8.63(5)}Sr_{2.37}Sb_{10}$ **(1)**						
*A*1 (Sr/Ca)	16*n*	.2522(2)	0	.1875(1)	21(1)	.35(1)/.65
*A*2 (Ca)	16*n*	.3398(2)	0	.3963(1)	20(1)	
*A*3 (Ca)	8*h*	.1681(5)	1681(5)	0	59(2)	
*A*4 (Sr)	4*e*	0	0	.3374(2)	21(1)	
Sb1	4*d*	.5000	0	.2500	14(1)	
Sb2	4*e*	0	0	.1283(1)	18(1)	
Sb3	16*m*	.2076(1)	.2076(1)	.3236(1)	19(1)	
Sb4	8*i*	.3447(1)	0	0	35(1)	
Sb5	8*h*	.1257(1)	.1257(1)	.5000	57(1)	
$Ca_{3.66(7)}Sr_{7.34}Sb_{10}$ **(2)**						
*A*1 (Sr)	16*n*	.2525(1)	0	.1881(2)	20(1)	
*A*2 (Sr/Ca)	16*n*	.3371(2)	0	.3973(2)	19(1)	.32(1)/.68
*A*3 (Sr/Ca)	8*h*	.1683(5)	.1683(5)	0	45(1)	.54(1)/.46
*A*4 (Sr)	4*e*	0	0	.3376(1)	20(1)	
Sb1	4*d*	.5000	0	.2500	12(1)	
Sb2	4*e*	0	0	.1266(1)	16(1)	
Sb3	16*m*	.2078(1)	.2078(1)	.3236(1)	19(1)	
Sb4	8*i*	.3495(1)	0	0	21(1)	
Sb5	8*h*	.1224(1)	.1224(1)	.5000	77(1)	

U_{eq} is defined as one third of the trace of the orthogonalized U_{ij} tensor.

full-matrix least-squares refinement on F^2 converged at $R_1 = 4.53\%$ and 3.69% for the observed data and $wR_2 = 9.88\%$ and 7.09% for all data for **(1)** and **(2)**, respectively. Bond valence sum analysis [25] carried out for all the alkaline-earth metal sites for **(1)** and **(2)** indicates all of the sites refined as mixed Ca/Sr sites to be correct. The values calculated from the refinement results are in good agreement with the formal oxidation states. However, bond valence calculations could not distinctively indicate the small amounts of vacancy for a particular site (~94% in case of *A*3).

Physical properties. Resistivities of powdered samples of nearly single phase samples of $Ca_{5.5}Sr_{5.5}Sb_{10}$ and $Ca_{3.5}Sr_{7.5}Sb_{10}$ (loaded compositions) sieved to a grain size between 150 and 250 μm and dispersed in chromatographic Al_2O_3 were measured by the *Q* method over a range of 110–294 K [26]. Magnetic susceptibility of these compositions was obtained at a field of 10 and 30 kOe over a range of 6–300 K with the aid of a Quantum design (MPMS) SQUID magnetometer. Samples were accurately weighed and were held between two fused silica rods within a tightly fitting outer silica tube and sealed under helium [27]. The raw data were corrected for the susceptibility of the container and the diamagnetic contributions of the ion cores. *M* vs. *H* data at 2 K indicated the absence of significant paramagnetic impurities. These graphical data are included in Supporting Information.

3. Results and discussion

A distinct size dependent crystallographic site preference of alkaline-earth metal ions in **(1)** and **(2)** shown by spheres shaded differently in Fig. 1(a) and (b) has been observed in this otherwise well defined $Ho_{11}Ge_{10}$ structure type [14,15]. Three discrete anionic species as has been noted earlier for this structure type is present which seems to be directing the site occupation of alkaline-earth metals. Sb_4 units (d(Sb–Sb) varying from 3.023(4) Å in **(2)** to 3.027(3) Å in **(1)**) are linked by cations three dimensionally through Sb_2 units (d(Sb–Sb) varying from 2.954(1) Å in **(1)** to 3.002(1) Å in **(2)**) units. These distances are similar in comparison with the previously reported examples [16,24]. Some important interatomic distances are given in Table 4. Thus no appreciable modification is observed in the Sb–Sb bonding distances both in Sb_4 rings as well as Sb_2 dumbbells. As both the end members of the series $Ca_{11-x}Sr_xSb_{10}$ are known to crystallize in the same structure type all the cation sites should be freely accessible to both the cations. However, a few cation sites were found to be occupied preferentially by either Ca or Sr. To the best of our knowledge, only one example for the mixed cation compound ($Sr_5Ba_6Sb_{10}$ [24]) crystallizing in $Ho_{11}Ge_{10}$ has been reported so far. Though no site preference for the cation site was discussed, the statistical mixing does indicate this preference. The most favorable position for the bigger Ba ions was the 4*e* site which in the present examples (1 and 2) is occupied by Sr ions (*A*4). This is followed by the occupation of the *A*1 (16*n*) sites, *A*3 (8*h*) and *A*2 (16*n*) sites which are occupied by approximately 70%, 60% and 15% of Ba in that order.

The remarkable consistency with which Sb_2 bonding distance has appeared across various examples in $M_{11}X_{10}$ (M = Ca, Sr, Eu, Yb; X = Sb, Bi) may lead one to believe that this is not effected by the lattice covalency to any good

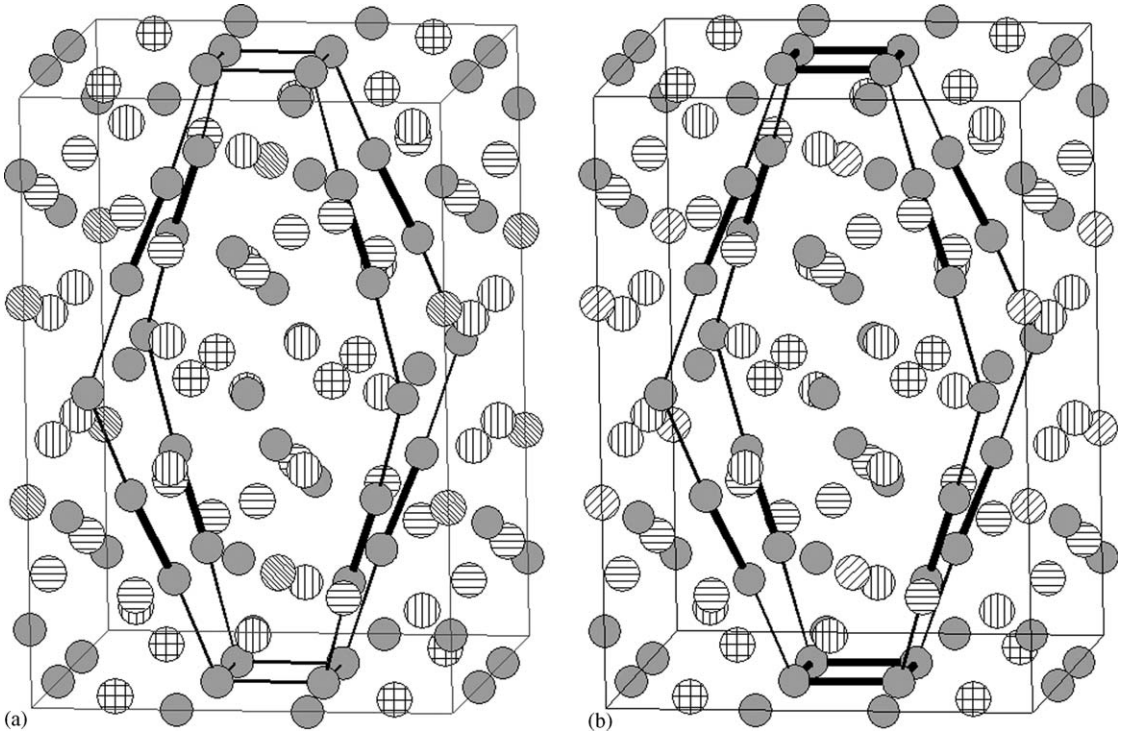

Fig. 1. ~[1 0 0] representation of unit cells of **(1)** (a) and **(2)** (b) phases. The short Sb–Sb distances are shown by thick bonds in both the figures. The grey spheres represent antimony, spheres with horizontal lines, vertical lines, cross and slanting lines represent *A*1, *A*2, *A*3 and *A*4 sites respectively.

Table 4
Important interatomic distances (Å)

Bond	$Ca_{8.63(5)}Sr_{2.37}Sb_{10}$	$Ca_{3.66(7)}Sr_{7.34}Sb_{10}$
Sb3–Sb3	2.954(1)	3.002(2)
Sb5–Sb5	3.026(3)	3.023(4)
Sb3–Sb5	3.388(2)	3.471(2)
Sb4–Sb4	3.740	3.717
Sb3–*A*1	3.494(1)/3.5610(8)	3.561(1)/3.6478(7)
Sb3–*A*2	3.226(1)	3.294(1)
Sb3–*A*3	3.743(4)	3.808(2)
Sb3–Sr2	3.544(1)	3.6377(9)

extent. Nevertheless, a progressive strengthening of Bi–Bi bonds in Bi_2 units was suggested on the basis of calculated overlap population in $M_{11}Bi_{10}$ [24] from Ca to Ba. This was suggested to be due to the decrease in electronegativities and the polarizing power of cations along the series. Contrary to the above a slight increase in the interatomic distance in the Sb dimers was noted for the Sr rich composition **(2)** in the present work. Fig. 2(a) shows the coordination around Sb3 along with the dimer. In both the structures, each Sb3 is surrounded by eight alkaline-earth metal cations along with two other Sb ions. In the Ca-rich phase all the alkaline-earth metal sites surrounding the dimer has mixed Ca and Sr occupancy whereas in the Sr rich phase these sites are occupied only by Sr suggesting that larger of the two cations are more favored (Fig. 2(a)). The coordination around Sb5 is shown in Fig. 2(b). Table 5 lists the number of nearest neighbors for all the antimony positions. As discussed earlier in the structural studies a unique feature of the $M_{11}Sb_{10}$ is the large thermal parameter of the Sb5 ion in all previous studies [16,24] and is also found in the ternary ($(Ca/Sr)_{11}Sb_{10}$) phases discussed here. The reason for high atomic displacement parameter for Sb5 may lie in its unique coordination environment. It may be noted that the Sb5 is surrounded by 7 alkaline-earth metal ions in contrast to 8 and 9 around Sb1 and Sb2 respectively which have the lowest thermal displacements. Four Sb ions in close proximity to Sb5 (along with the 7 alkaline-earth ions) would lead to a lower covalency which in turn would drive Sb towards anion–anion bonding. As mentioned earlier a slight increase (~.05 Å) in interatomic distance in the Sb dimer (Sb3–Sb3) was noted in **(2)**. This can be attributed to an increase in one of the Sb3–*A*1 distances (Table 4**)**. Whether or not the reason lies in the Sb–Sb dimers, the larger cations preferentially occupy sites which are closer to the diantimony ions with the exception of the 4*e* site which is exclusively occupied by strontium in both **(1)** and **(2)**. This could however be attributed to the greater coordination number around this site. A more comprehensive understanding of these site preferences can be had by comparing the coordination polyhedra around each alkaline-earth metal site. Fig. 3 (arranged according to site preference) shows the comparison of nearest neighbors (drawn at 4 Å) around alkaline-earth metals in both these structures. The 9-coordinated *A*1 (4*e*) site provides the most favorable coordination for the larger cation (Ba is favored over Sr [24] which is favored over Ca (present work)) **(**Fig. 3a**)**. The

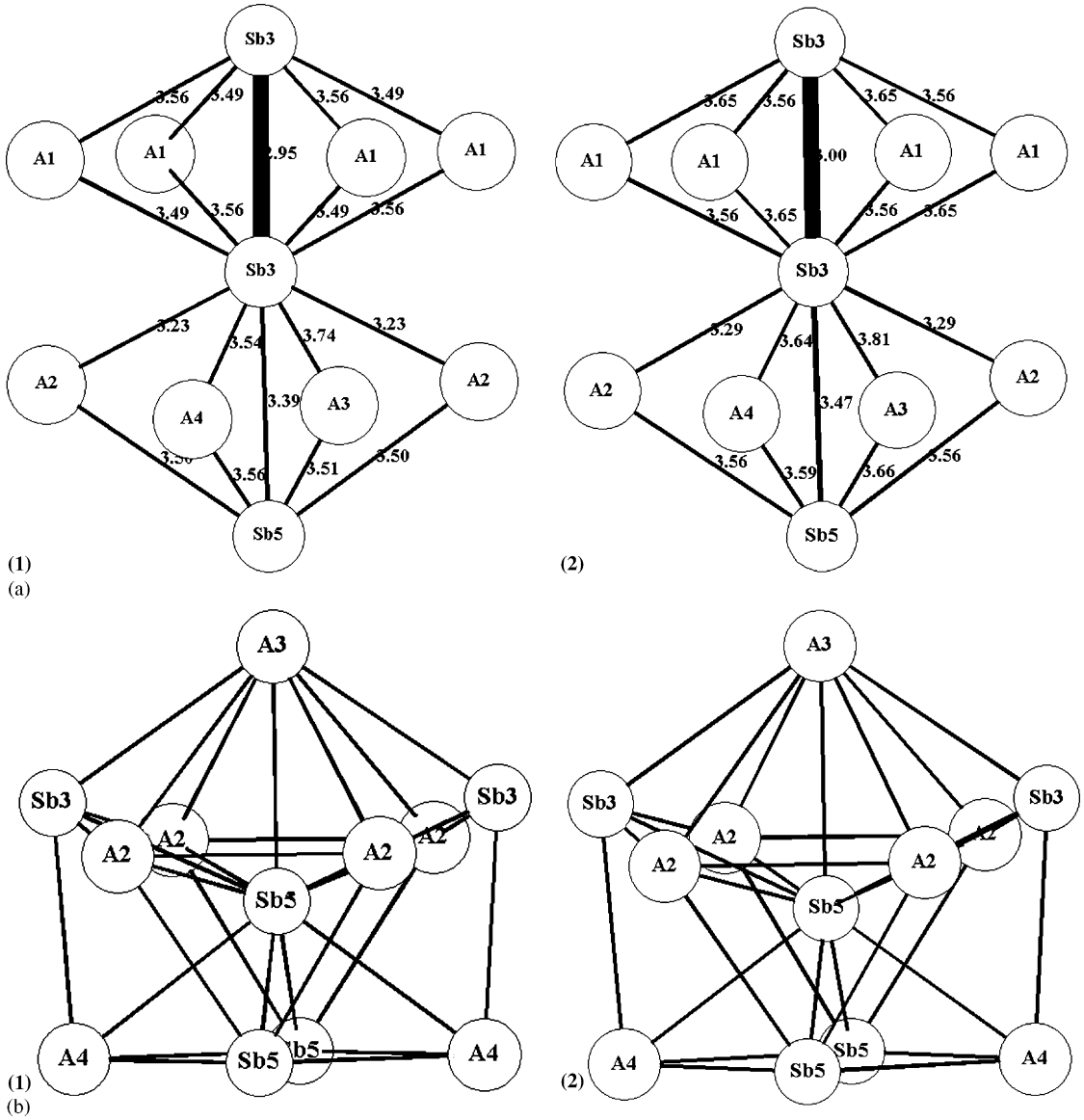

Fig. 2. (a) Coordination around Sb3–Sb3 dimers in **(1)** and **(2)**; (b) coordination around Sb5 in **(1)** and **(2)**.

Table 5
Number of nearest neighbors around Sb

Atom	Neighbors		
	Alkaline-earth metal	Antimony	Total
Sb1	8	0	8
Sb2	9	0	9
Sb3	8	2	10
Sb4	8	1	9
Sb5	7	4	11

next favored site for Sr, as indicated by the respective occupancies of Ca and Sr ions, is the *A*1 (16*n*) site **(**Fig. 3b**)**. The pentagonal bipyramidal coordination of this site is the same as that of the 8*h* site (Fig. 3c**)**. However the coordination around the former (16*n*) site involves two Sb_2 dimers constituting a pentagon. There is a slight deviation from planarity, with the metal cation at the center (Sr/Ca) not in the plane of the pentagon. In contrast, in the 8*h* site, the Sb ions constituting the pentagon are planar with the alkaline-earth metal ion lying in the plane. With this arrangement the former site seems to be providing a better coordination for the larger cations. The variation in Sb5–Sb3 distance (Table 4) is in line with the reported values in $Ca_{11}Sb_{10}$ and $Sr_{11}Sb_{10}$ (3.363 and 3.603(8) Å, respectively) and increases with increasing cation size. Our observations regarding Sb_2 interatomic distance is however in contrast to the previous reports [16,24]. We observed an increase of ~.05 Å in **(2)** compared to **(1)** on increasing the Sr content from 22% to 68% which is in accordance with the increase in the lattice parameters. However, previous reports have indicated a reduction by ~.01 Å of the Sb3–Sb3 dimer distance in pure Sr compound ($Sr_{11}Sb_{10}$) compared to the pure Ca compound ($Ca_{11}Sb_{10}$).

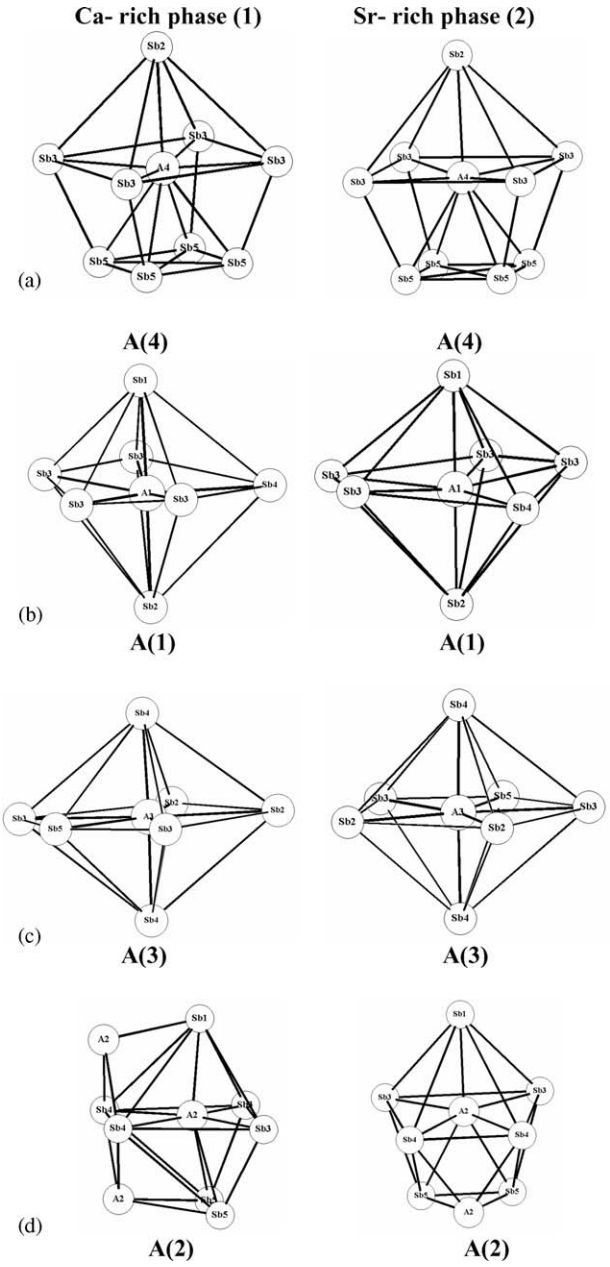

Fig. 3. Comparison of alkaline-earth metal coordination in **(1)** and **(2)** drawn at 4 Å.

The Q-measurements on nearly single-phase samples of $Ca_{5.5}Sr_{5.5}Sb_{10}$ and $Ca_{3.5}Sr_{7.5}Sb_{10}$ (loaded compositions) indicated the compounds to be non-metallic. The magnetic susceptibility data (Supporting Information) showed $Ca_{3.5}Sr_{7.5}Sb_{10}$ to be diamagnetic (M/H at 30 kOe equal to about -3.5×10^{-5} emu/mole over ~100–350 K) with no significant paramagnetic impurity. $Ca_{5.5}Sr_{5.5}Sb_{10}$ shows a very low value (5.5×10^{-4} emu/mole) of temperature independent magnetic susceptibility (~100–350 K) at 30 kOe. These phases can thus be classified as ideal Zintl phase as indicated by the formal oxidation state assignments: 44 $(Ca/Sr)^{2+}$, $2Sb_4^{4-}$, $8Sb_2^{4-}$ and $16Sb^{3-}$ (for a unit cell, $Z=4$).

Acknowledgments

The authors thank Professor J.D. Corbett, Iowa State University, for supporting (from his NSF Grant DMR-0129785) the visit of A.K.G. and S.G. to ISU and Ames Laboratory where part of this research was carried out. The authors also thank Department of Science and Technology, Government of India and IIT Delhi for funding of the Bruker SMART APEX X-ray diffractometer. We are also indebted to Serge Bud'ko for the susceptibility data.

Supporting information available. For tables of more detailed crystal and structural refinement data and anisotropic displacement ellipsoids for the two structures; two figures of magnetic susceptibility data see Appendix A.

Appendix A. Supplementary materials

Supplementary data associated with this article can be found in the online version at doi:10.1016/j.jssc.2006.03.027.

References

[1] J.D. Corbett, Angew. Chem. Int. Ed. 39 (2000) 670.
[2] J.D. Corbett, in: S. Kauzlarich (Ed.), Chemistry, Structure and Bonding of Zintl Phases and Ions, VCH, New York, 1996 [Chapter 3].
[3] H. Schaefer, Annual Review of Materials Science 15 (1985) 1.
[4] R. Nesper, Prog. Solid State Chem. 20 (1990) 1.
[5] R. Nesper, Angew Chem. Int. Ed. Eng. 30 (1991) 789.
[6] J.D. Corbett, Chem. Rev. 85 (1985) 383.
[7] S.C. Sevov, J.D. Corbett, Inorg. Chem. 30 (1991) 4875.
[8] Z.-C. Dong, J.D. Corbett, J. Am. Chem. Soc. 116 (1994) 3429.
[9] A.K. Ganguli, J.D. Corbett, M. Köckerling, J. Am. Chem. Soc. 120 (1998) 1223.
[10] G.A. Papoian, R. Hoffmann, Angew. Chem. Int. Ed. 39 (2000) 2408.
[11] A.M. Mills, R. Lam, M.J. Fergusan, L. Deakin, A. Mar, Coord. Chem. Rev. 207 (2002) 233.
[12] F. Gascoin, S. Ottensmann, D. Stark, S.M. Haile, G.J. Snyder, Advanced Functional Materials 15 (2005) 1860.
[13] E. Dashjav, A. Szczepenowska, H. Kleinke, J. Mater. Chem. 12 (2002) 345.
[14] G.S. Smith, Q. Johnson, A.G. Tharp, Acta Cryst 23 (1967) 640.
[15] K. Deller, B. Eisenmann, Z. Naturforsch, Teil B 31 (1976) 29.
[16] A. Rehr, S.M. Kauzlarich, Acta Cryst. C 50 (1994) 1859.
[17] A.K. Ganguli, S. Gupta, J.D. Corbett, Inorg. Chem. 45 (2006) 196.
[18] R. Schmelczer, D. Schwarzenbach, F. Hulliger, Z. Naturforsch, Teil B 34 (1979) 1213.
[19] H.L. Clark, H.D. Simpson, H. Steinfink, Inorg. Chem. 9 (1970) 1962.
[20] A.K. Ganguli, S. Gupta, J.-T. Zhao, E.-A. Leon-Escamilla, J.D. Corbett, J. Solid State Chem. 178 (2005) 2965.
[21] E.A. Leon-Escamilla, W.-M. Hurng, E.S. Peterson, J.D. Corbett, Inorg. Chem. 36 (1997) 703.
[22] SMART, Bruker AXS, Inc., Madison, WI, 1996.
[23] SHELXTL, Bruker AXS, Inc., Madison, WI, 2000.
[24] G. Derrien, M. Tillard-Charbonnel, A. Manteghetti, L. Monconduit, C. Belin, J. Solid State Chem. 164 (2002) 169.
[25] I.D. Brown, Acta Crystallorg. B. 41 (1985) 244.
[26] J.T. Zhao, J.D. Corbett, Inorg. Chem. 34 (1995) 378.
[27] S.C. Sevov, J.D. Corbett, Inorg. Chem. 31 (1992) 1895.